



A Journal of



Accepted Article

Title: Synthesis, characterization and heterogeneous catalytic activity of sulfamic acid functionalized magnetic IRMOF-3

Authors: Mohammad Mahdi Mostafavi and Farnaz Movahedi

This manuscript has been accepted after peer review and appears as an Accepted Article online prior to editing, proofing, and formal publication of the final Version of Record (VoR). This work is currently citable by using the Digital Object Identifier (DOI) given below. The VoR will be published online in Early View as soon as possible and may be different to this Accepted Article as a result of editing. Readers should obtain the VoR from the journal website shown below when it is published to ensure accuracy of information. The authors are responsible for the content of this Accepted Article.

To be cited as: *Eur. J. Inorg. Chem.* 10.1002/ejic.201801054

Link to VoR: <http://dx.doi.org/10.1002/ejic.201801054>

WILEY-VCH

Synthesis, characterization and heterogeneous catalytic activity of sulfamic acid functionalized magnetic IRMOF-3

Mohammad Mahdi Mostafavi and Farnaz Movahedi*

Department of Chemistry and Petrochemical Engineering, Standard Research Institute, P.O. Box 31745-139, Karaj, Iran

Abstract

Here in, post-synthesis modification of $\text{Fe}_3\text{O}_4/\text{IRMOF-3}$ nanocomposite with chlorosulfonic acid groups afforded sulfamic acid-functionalized magnetic metal-organic frameworks ($\text{Fe}_3\text{O}_4/\text{IRMOF-3}/\text{SO}_3\text{H}$). Functionalization was followed through FT-IR, XRD, TGA, BET, FE-SEM/EDS and elemental analyses. The catalytic efficiency of the as prepared nanocomposite was evaluated through one-pot pseudo four-component reaction of secondary amines, malononitrile and salicylaldehydes in EtOH under mild conditions. Magnetic tendency of the functionalized IRMOF-3, made simple decantation by external magnetic field from the reaction mixture, continued with catalyst reuse for at least five times without significant loss of catalytic efficiency.

Introduction

The use of multicomponent reactions (MCRs) strategy leading to the construction of novel and complex molecular structures in comparison to conventional multi-step synthesis, is fascinating for the scientific community.^[1-3] The virtues of procedure simplicity, reduction of time, energy and costs, and avoidance of time-consuming expensive purification processes^[4,5] play decisive roles. On the other hand, Bronsted acids are general catalysts in various organic reactions because of their good reactivity and selectivity in catalysis fields.^[6] However, there are some disadvantages in using homogeneous Bronsted acid catalysts, such as difficulties in their separation, recovery and recycling, environmental pollution and intense corrosion of equipment.^[7] Recently, some kind of heterogeneous Bronsted acid catalysts, in which can be reached through the chemical cross-linking of acid resources with solid phase supports, such as phenylsulfonic acid and tungstic acid groups with mesoporous SBA-15,^[8,9] and sulfonic acid groups with Fe_3O_4 magnetic nanoparticles and MCM-41^[10-12] have represented numerous advantages over homogeneous catalysts in the aspect of recovery and recycling to put forward the MCRs.

In recent years a considerable attention to porous coordination polymers or metal-organic frameworks (MOFs) has been focused within a relatively short time-frame.^[13] The current uses and the possible future applications of MOFs, including separation,^[14] storage^[15,16] optical devices^[17] drug delivery,^[18,19] luminescence,^[20] etc. have attracted significant research attention in this wide scientific field. Because of the porosity in structure, large surface area and highly tailorable properties,

* Corresponding author Tel.: +98-912-7031230; Fax: +98-26-32803880; E-mail: Fzmovahedi@yahoo.com, Homepage URL: en.standard.ac.ir/Farnaz_Movahedi_cv.aspx

MOFs have interesting potential to be used as heterogeneous Brønsted acid catalysts in organic synthesis, even though few successful Brønsted acid-MOFs have been reported in recent years.^[21-23] Accordingly, post-synthesis and employing of MOFs as supporting phase with the other functional groups would be desirable for preparation of specific MOFs with excessive catalytic potential. The post-synthetic modification (PSM) of MOFs introduces a highly desirable method by attaching various catalytic centers through stable covalent bonds in order to form a wide range of stronger Brønsted acidic functionalized MOFs.^[24-26] Also anchoring of magnetic compounds such as Fe₃O₄ magnetic nanoparticles into MOFs scaffold involves great advantages from the point of separation in comparison with the other methods.^[27]

Benzopyranopyrimidines have gained much attention in recent years due to their inherent and various pharmacological potential such as analgesic, in vivo antitumor, anti-inflammatory and anti-aggregating activities.^[28-31] These compounds are considered as a class of important medicinal scaffolds that are commonly derived from the condensation reaction of salicylaldehydes, malononitrile and secondary amines in the presence of acid catalysts. Recently, ionic liquids, LiClO₄, ZrOCl₂, manganese oxide salen complex immobilized on Fe₃O₄ magnetic nanoparticles and microwave irradiation have been utilized for their synthesis.^[32-35]

In 2013, we investigated the capability of one-pot multicomponent synthesis of benzopyranopyrimidine derivatives in the presence of silica nanoparticles immobilized benzoylthiourea ferrous complex as a catalyst in EtOH at room temperature.^[36] Following our previous researches on multicomponent reactions,^[37,38] here in, we report a novel approach for the synthesis of benzopyranopyrimidine derivatives using sulfamic acid functionalized magnetic IRMOF-3. For this purpose, a facile fabrication of Fe₃O₄/IRMOF-3 nanocomposite is presented through preparation of IRMOF-3 in the presence of amino-modified Fe₃O₄@SiO₂ NPs by a solvothermal method. Afterwards sulfamic acid-functionalized Fe₃O₄/IRMOF-3 was prepared by a post-functionalization strategy. The obtained Fe₃O₄/IRMOF-3/SO₃H was systematically characterized and its catalytic efficiency was evaluated for the one-pot pseudo four-component synthesis of benzopyranopyrimidines.

Results and discussion

Characterization of Fe₃O₄/IRMOF-3/SO₃H

The X-ray diffraction pattern of the as-prepared Fe₃O₄@SiO₂ is shown in Fig. 1a. The relative intensities and positions of the peaks confirmed well with a cubic spinel magnetic structure (JCPDS No. 19-0629).^[39] On the other hand, the X-ray diffraction patterns of the IRMOF-3 are shown before and after post synthetic modification with Fe₃O₄ and chlorosulfonic acid (Fig. 1b, 1c). The reflections peaks around $2\theta = 6.8^\circ$ and 9.6° indicate that a desirable crystalline material was produced (Fig. 1b).^[40,41] Also the Fe₃O₄/IRMOF-3/SO₃H (Fig. 1c) exhibited the same characteristic peaks as the unmodified IRMOF-3. The XRD results obtained from the reused catalyst showed that the overall structure of the catalyst could be retained even after 5th run during the reactions.

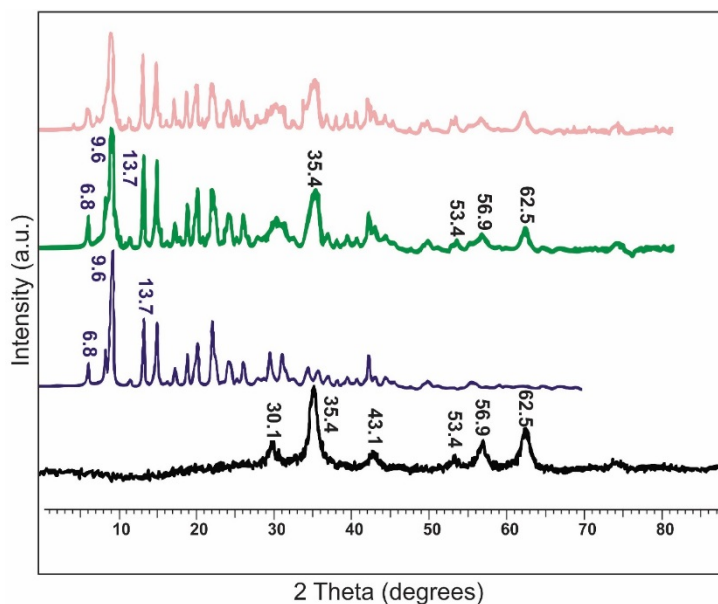


Fig. 1. XRD patterns of (a) $\text{Fe}_3\text{O}_4@\text{SiO}_2$, (b) IRMOF-3, (c) $\text{Fe}_3\text{O}_4/\text{IRMOF-3}/\text{SO}_3\text{H}$ and (d) reused $\text{Fe}_3\text{O}_4/\text{IRMOF-3}/\text{SO}_3\text{H}$.

The FT-IR spectra of the $\text{Fe}_3\text{O}_4@\text{SiO}_2$ MNPs, IRMOF-3 and $\text{Fe}_3\text{O}_4/\text{IRMOF-3}/\text{SO}_3\text{H}$ nanocomposite are shown in Fig. 2. The peaks at 575 and 1085 cm^{-1} are ascribed to Fe-O and O-Si-O stretching vibrations, respectively (Fig. 2a). The spectra of the IRMOF-3 exhibited a strong peak at 1573 cm^{-1} , indicating the deprotonation of -COOH groups in 2-aminoterephthalic acid upon the reaction with metal ions (Fig. 2b). In addition, two peaks at 3358 and 3475 cm^{-1} due to the N-H stretching vibration of the amine functionalities and the peak at 1256 cm^{-1} related to the C-N vibrations are assigned, respectively.^[42] In $\text{Fe}_3\text{O}_4/\text{IRMOF-3}/\text{SO}_3\text{H}$ (Fig. 2c) two new bands are appeared at 1282 and 1151 cm^{-1} , which would be ascribed to the O=S=O asymmetric and symmetric stretching modes, respectively, and the peak at 1093 cm^{-1} which would be assigned to S-O stretching vibration. Also the peak near 3500 cm^{-1} was probably attributed to the NH groups, which was overlapped by the O-H stretching vibrations. As a result, all of these evidences confirm successful modification of the amines to sulfamic acid groups.

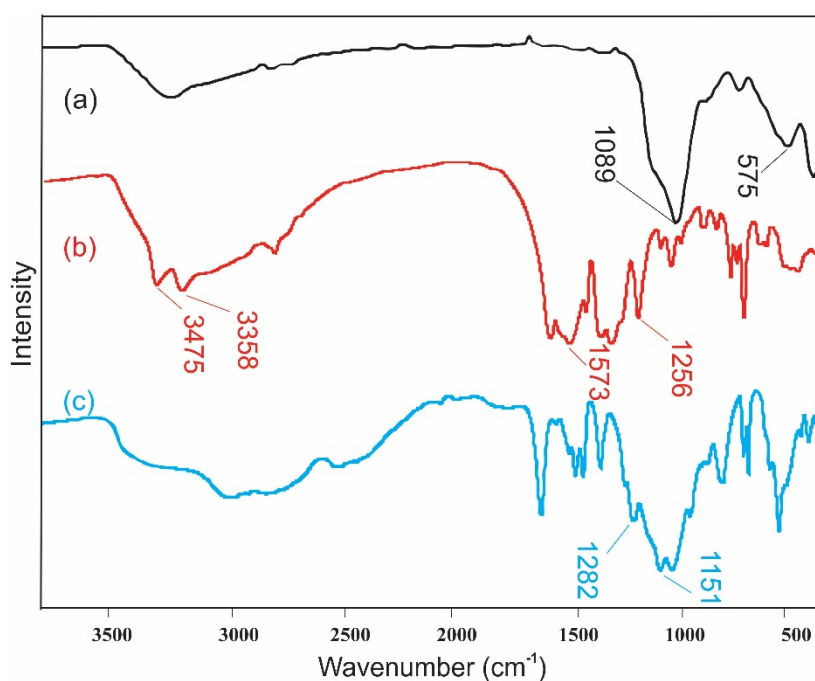


Fig. 2. FT-IR spectra of (a) $\text{Fe}_3\text{O}_4@\text{SiO}_2$, (b) IRMOF-3, and (c) $\text{Fe}_3\text{O}_4/\text{IRMOF-3}/\text{SO}_3\text{H}$.

To evaluate the morphology of IRMOF-3 and $\text{Fe}_3\text{O}_4/\text{IRMOF-3}/\text{SO}_3\text{H}$, the prepared samples were investigated by FESEM (Fig. 3). The Fe_3O_4 NPs have spherical shape ordered with an average size of 37 nm (Fig. 3a). As it is shown (Fig. 3b and 3c), the IRMOF-3 and $\text{Fe}_3\text{O}_4/\text{IRMOF-3}/\text{SO}_3\text{H}$ have an acceptable crystalline structure, and Fe_3O_4 MNPs are well dispersed within the network homogeneously, due to the electrostatic interactions between the Fe_3O_4 NPs owning negative charges and IRMOF-3 with positive charges.^[43] Also, the post modification of $\text{Fe}_3\text{O}_4/\text{IRMOF-3}$ with chlorosulfonic acid groups seems not to interfere in the crystalline structure of IRMOF-3 (Fig. 3c), which is in accordance with the XRD results. Also the elemental composition of $\text{Fe}_3\text{O}_4/\text{IRMOF-3}/\text{SO}_3\text{H}$ nanocomposite was determined by SEM-EDS (Fig. 3d). It shows a generic spectrum with separate peaks from C, N, Si, Zn, S, O and Fe, in which was used to determine the relative elemental analysis. The quantitative analysis of N and S gives weight ratios of 4.21% and 9.85%, respectively, with a loading at ca. 2.99 mmol/g for N and 3.07 mmol/g for S. The results show that all of the amine groups in IRMOF-3 structure were modified successfully with chlorosulfonic acid groups. Finally, individual weight percent of each component in functionalized magnetic IRMOF-3 was estimated 8.12% for Fe_3O_4 , 7.96% for SiO_2 , 59.03% for MOF and 24.88% for $-\text{SO}_3\text{H}$, approximately.

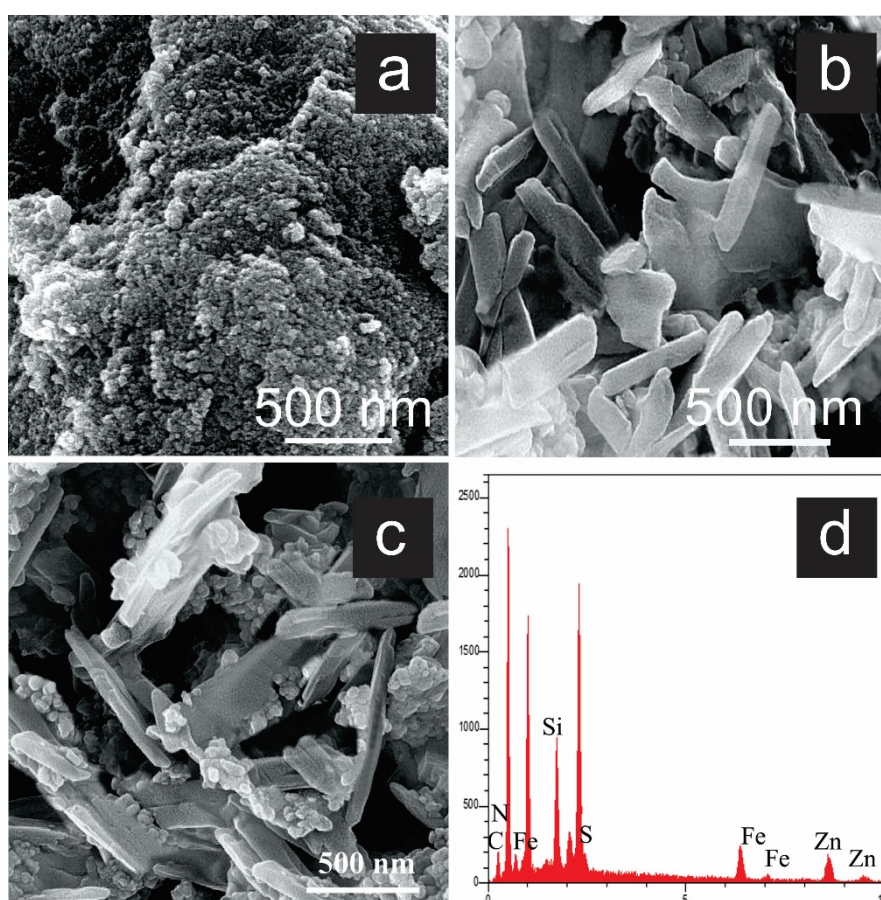


Fig. 3. The FESEM images of (a) Fe_3O_4 NPs, (b) IRMOF-3, (c) $\text{Fe}_3\text{O}_4/\text{IRMOF-3}/\text{SO}_3\text{H}$, and (d) SEM-EDS analysis.

On the other hand, the number of H^+ determined by acid-base titration was 2.93 mmol g^{-1} that this value is close to the EDS results for the sulfur content (3.07 mmol g^{-1}). It was concluded that most of sulfur species on the surface of the $\text{Fe}_3\text{O}_4/\text{IRMOF-3}/\text{SO}_3\text{H}$ nanocomposite are in the form of sulfamic acid groups. It is noteworthy that the total concentration of H^+ for unmodified $\text{Fe}_3\text{O}_4/\text{IRMOF-3}$ was not placed on detection range by titration and it was resulted that the acidity of $\text{Fe}_3\text{O}_4/\text{IRMOF-3}/\text{SO}_3\text{H}$ is caused by the sulfamic acid groups.

The BET surface area and pore volume were calculated using the N_2 adsorption and the pore size distribution pattern calculated from desorption branch of the N_2 isotherm by Barrett-Joyner-Halenda (BJH) model (Fig. 4). The IRMOF-3 nanocomposite exhibit a typical type I isotherm (Fig. 4a, 4b), with a distinct hysteresis loop above 0.8 of P/P_0 in desorption

branch for Fig. 4a, indicating the presence of mesoporosity. Comparatively, both the pore volume and specific surface area have large decrease after the incorporating of the $-\text{SO}_3\text{H}$ groups into the $\text{Fe}_3\text{O}_4/\text{IRMOF-3}$. In the case of Langmuir surface area, the N_2 adsorption revealed a decrease after post modification of $\text{Fe}_3\text{O}_4/\text{IRMOF-3}$ to $\text{Fe}_3\text{O}_4/\text{IRMOF-3}/\text{SO}_3\text{H}$ from ca. $400 \text{ m}^2/\text{g}$ to $70 \text{ m}^2/\text{g}$ and the average pore volume decreased from $0.52 \text{ cm}^3/\text{g}$ to $0.08 \text{ cm}^3/\text{g}$, respectively. Obviously, the inclusion of the $-\text{SO}_3\text{H}$ groups into the nanocages would be responsible for such a decrease. Similar results are reported previously for modification of the IRMOF-3.^[44] As can be seen from Fig. 4c and 4d, the pore-size distribution of the as-prepared magnetic IRMOF-3 and $\text{Fe}_3\text{O}_4/\text{IRMOF-3}/\text{SO}_3\text{H}$ nanocomposites from the desorption branch of the N_2 isotherm by BJH model was calculated 8.0 nm and 5.4 nm , respectively.

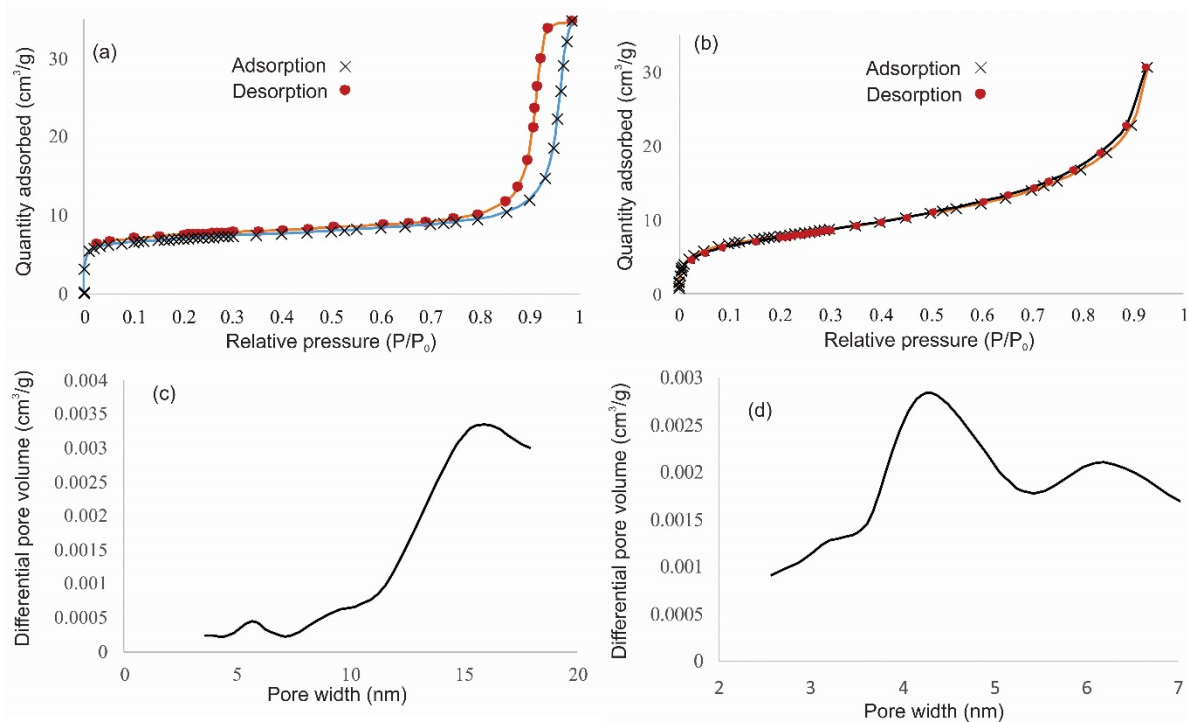


Fig. 4. N_2 adsorption–desorption isotherms of (a) $\text{Fe}_3\text{O}_4/\text{IRMOF-3}$ and (b) $\text{Fe}_3\text{O}_4/\text{IRMOF-3}/\text{SO}_3\text{H}$, the BJH pore size distributions of (c) $\text{Fe}_3\text{O}_4/\text{IRMOF-3}$ and (d) $\text{Fe}_3\text{O}_4/\text{IRMOF-3}/\text{SO}_3\text{H}$.

Thermogravimetric analysis (TGA) of IRMOF-3 and $\text{Fe}_3\text{O}_4/\text{IRMOF-3}/\text{SO}_3\text{H}$ was investigated under N_2 flow and running from room temperature to $600 \text{ }^\circ\text{C}$ (Fig. 5.). IRMOF-3 showed two steps weight loss, first weight loss of about $8 \text{ wt } \%$ below $170 \text{ }^\circ\text{C}$ due to the removing of the remaining trapped solvent, and a second weight loss of $42 \text{ wt } \%$ due to the decomposition of organic linkers between 350 and $550 \text{ }^\circ\text{C}$. The $\text{Fe}_3\text{O}_4/\text{IRMOF-3}/\text{SO}_3\text{H}$ revealed the same thermal behavior as IRMOF-3 before $170 \text{ }^\circ\text{C}$ but it showed sensible differences versus IRMOF-3 with an excess weight loss ($\sim 10 \text{ wt } \%$) between 250 and $350 \text{ }^\circ\text{C}$, that is likely due to the thermal crystal phase transformation from Fe_3O_4 to $\gamma\text{-Fe}_2\text{O}_3$ ^[45] and breakdown of the sulfamic acid functionalities, indicating that the $\text{Fe}_3\text{O}_4/\text{IRMOF-3}/\text{SO}_3\text{H}$ is stable only up to $250 \text{ }^\circ\text{C}$.

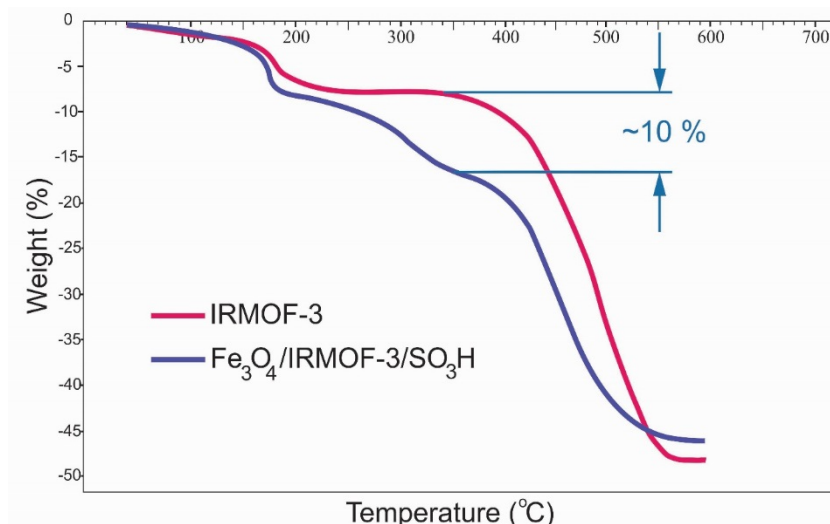


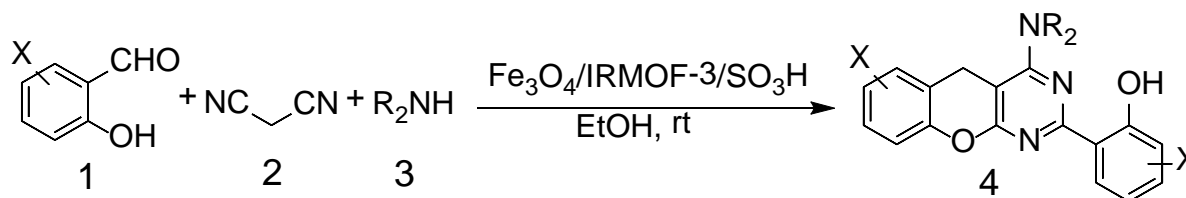
Fig. 5. TGA analysis of $\text{Fe}_3\text{O}_4/\text{IRMOF-3}/\text{SO}_3\text{H}$ vs. IRMOF-3.

Catalytic activity of $\text{Fe}_3\text{O}_4/\text{IRMOF-3}/\text{SO}_3\text{H}$ nanocomposite

Catalytic activity of $\text{Fe}_3\text{O}_4/\text{IRMOF-3}/\text{SO}_3\text{H}$ nanocomposite was explored for the one-pot pseudo four-component condensation reaction of salicylaldehydes, malononitrile and secondary amines for synthesis of the benzopyranopyrimidines (Scheme 1). For this purpose, various reaction conditions were appraised by salicylaldehyde, malononitrile, and morpholine as a model test reaction (3j) and the results are summarized in Table 1. $\text{Fe}_3\text{O}_4/\text{IRMOF-3}$ and IRMOF-3 catalyzed the reaction with 20% and 10% yields, respectively (Table 1, entries 8 and 9). In the presence of Fe_3O_4 MNPs only trace amounts of the product was accomplished, while under catalyst-free conditions, the reaction did not proceed anyway (Table 1, entries 10 and 15). Nevertheless, the modified catalyst, *i.e.* $\text{Fe}_3\text{O}_4/\text{IRMOF-3}/\text{SO}_3\text{H}$ increased the yield up to 95% (Table 1, entry 7).

In order to select the most suitable media, the model reaction was performed in various solvents in the presence of $\text{Fe}_3\text{O}_4/\text{IRMOF-3}/\text{SO}_3\text{H}$ (10 mg per 1mmol of reactants) as the catalyst (Table 1, entries 1-7). Clearly, using polar protic solvents such as EtOH, MeOH and H_2O led to higher yields 80-98% (Table 1, entries 1, 3, 7), while the reaction did not proceed using nonpolar or polar aprotic solvents such as *n*-Hexane and THF (Table 1, entries 4, 5). Besides, in the solvent-free conditions, the reaction did not achieve reasonable yields (Table 1, entry 6).

In order to study the effect of the catalyst concentration, the reaction proceeded using different amounts of the $\text{Fe}_3\text{O}_4/\text{IRMOF-3}/\text{SO}_3\text{H}$ under constant reaction conditions. Increasing the quantity of the catalyst from 5 mg to 10 mg led to an increase in the yield of the model reaction. However, we found only 10 mg catalyst is enough to catalyze the reaction up to high yields and using more amounts of the catalyst did not raise the yields to an appreciable extent (Table 1, entries 11-14).



Scheme 1. One-pot pseudo four-component synthesis of benzopyranopyrimidines promoted by $\text{Fe}_3\text{O}_4/\text{IRMOF-3}/\text{SO}_3\text{H}$.

Table 1. Optimization of the $\text{Fe}_3\text{O}_4/\text{IRMOF-3}/\text{SO}_3\text{H}$ catalyzed model reaction (3j) for the α -amino nitrile synthesis.^a

Entry	Catalyst	Solvent	Yield (%) ^b
1	$\text{Fe}_3\text{O}_4/\text{IRMOF-3}/\text{SO}_3\text{H}$ (10 mg)	H_2O	80
2	$\text{Fe}_3\text{O}_4/\text{IRMOF-3}/\text{SO}_3\text{H}$ (10 mg)	CH_2Cl_2	40
3	$\text{Fe}_3\text{O}_4/\text{IRMOF-3}/\text{SO}_3\text{H}$ (10 mg)	MeOH	90

4	Fe ₃ O ₄ /IRMOF-3/SO ₃ H (10 mg)	THF	-
5	Fe ₃ O ₄ /IRMOF-3/SO ₃ H (10 mg)	n-Hexane	-
6	Fe ₃ O ₄ /IRMOF-3/SO ₃ H (10 mg)	Solvent-free	20
7	Fe ₃ O ₄ /IRMOF-3/SO ₃ H (10 mg)	Ethanol	95
8	Fe ₃ O ₄ /IRMOF-3 (10 mg)	Ethanol	20
9	IRMOF-3 (10 mg)	Ethanol	10
10	Fe ₃ O ₄ MNPs (10 mol%)	Ethanol	5
11	Fe ₃ O ₄ /IRMOF-3/SO ₃ H (5 mg)	Ethanol	90
12	Fe ₃ O ₄ /IRMOF-3/SO ₃ H (10 mg)	Ethanol	95, 95, 93 ^c
13	Fe ₃ O ₄ /IRMOF-3/SO ₃ H (15 mg)	Ethanol	95
14	Fe ₃ O ₄ /IRMOF-3/SO ₃ H (20 mg)	Ethanol	95
15	No Catalyst	Ethanol	-

^a Reaction conditions: salicylaldehyde (2 mmol), morpholine (1 mmol), malononitrile (1 mmol), catalyst, solvent (4 mL), room temperature.

^b Isolated yields.

^c Yields in rt, 40 °C, and 70 °C.

The substitution effect was investigated by employing various derivatives of salicylaldehydes and secondary amines under the optimized reaction conditions, and the results are summarized in Table 2. The reaction can tolerate a wide variety of salicylaldehyde derivatives carrying either electron-donating substituents such as methoxy group, and electron-withdrawing groups such as halogens. In addition, aliphatic amines such as diethylamine and dimethylamine react as well as aromatic amines. However the best yields were achieved with cyclic secondary amines such as morpholine, piperidine and 4-Methyl piperidine. All products are known compounds,^[36,46] and found to be identical with authentic samples through melting points and spectroscopic data. Almost all the reactions worked quite well and the desired products were obtained in good to high yields and reasonable turnover numbers (TON) within sustainable reaction times. The TON, defined as moles of product produced per mole of active site of catalyst (H⁺).

In order to achieve relatively high yields at optimized conditions, the temperature effect was examined at room temperature (rt), 40 °C, and 70 °C. As shown in Table 1 (entry 12), by increasing the temperature from ambient temperature to 40 °C, the conversion rate didn't increase at all. However, a decrease in yield was observed when temperature increased from 40 °C to 70 °C. Then, ambient temperature was chosen as the optimum circumstance for the reaction.

Due to importance of the recyclability and the reusability of catalysts in organic reactions, the catalytic activity of the recycled Fe₃O₄/IRMOF-3/SO₃H was explored in this system. For this purpose, in each run after 1 h, the catalyst was separated from the model reaction mixture (3j) by a simple magnetic decantation. The separated catalyst was washed with methanol several times, dried under vacuum at 90 °C, and then was reused in subsequent cycle. The results showed (Table 2, entry 10) that the nanocomposite could be successfully used for at least five consecutive runs without significant loss of its catalytic activity. Also to test for leaching of the catalyst, the model test reaction was carried out in presence of the Fe₃O₄/IRMOF-3/SO₃H (10 mg) and at the point that yield was 45%, the catalyst was filtered in hot EtOH. The mother liquor transferred to another screw cap test tube and the reaction procedure allowed to be continued at ambient temperature, although no further remarkable conversation was observed. On the basis of the obtained results, no significant active species from the solid catalyst migrates to the supernatant and the catalysis is truly heterogeneous.

Table 2. The pseudo four-component reaction of salicylaldehydes, malononitrile and secondary amines catalyzed by Fe₃O₄/IRMOF-3/SO₃H under ambient conditions.^a

Entry	Aldehyde	Secondary amine	Product	Yields (%)	TON ^b
1	salicylaldehyde	N-Methylaniline	3a	83	108
2	salicylaldehyde	N-Eethylaniline	3b	80	108
3	5-Chlorosalicylaldehyde	Dimethylamine	3c	90	119
4	salicylaldehyde	Dimethylamine	3d	92	100
5	5-Methoxysalicylaldehyde	Dimethylamine	3e	87	112
6	5-Chlorosalicylaldehyde	Diethylamine	3f	78	111
7	salicylaldehyde	Diethylamine	3g	83	98
8	5-Methoxysalicylaldehyde	Diethylamine	3h	85	118
9	salicylaldehyde	Pyrrolidine	3i	95	112
10	salicylaldehyde	Morpholine	3j	95(95,94,94,93) ^c	117
11	5-Chlorosalicylaldehyde	Pyrrolidine	3k	95	134
12	5-Chlorosalicylaldehyde	Morpholine	3l	94	138
13	5-Methoxysalicylaldehyde	Pyrrolidine	3m	98	135
14	5-Methoxysalicylaldehyde	Morpholine	3n	97	139
15	salicylaldehyde	4-Methyl piperidine	3o	95	121
16	5-Chlorosalicylaldehyde	4-Methyl piperidine	3p	92	139
17	5-Methoxysalicylaldehyde	4-Methyl piperidine	3q	98	145
18	3,5-Dichlorosalicylaldehyde	4-Methyl piperidine	3r	95	165

19	3,5-Dichlorosalicylaldehyde	Diethylamine	3s	80	132
20	5-bromosalicylaldehyde	Dimethylamine	3t	90	146
21	3,5-Dichlorosalicylaldehyde	Morpholine	3u	94	160

^a Reaction conditions: aldehyde (2 mmol), secondary amine (1 mmol), malononitrile (1 mmol), catalyst (10 mg), EtOH (4 mL), room temperature.

^b Turnover number: number of moles of product per mole of active site of catalyst (mole of H⁺).

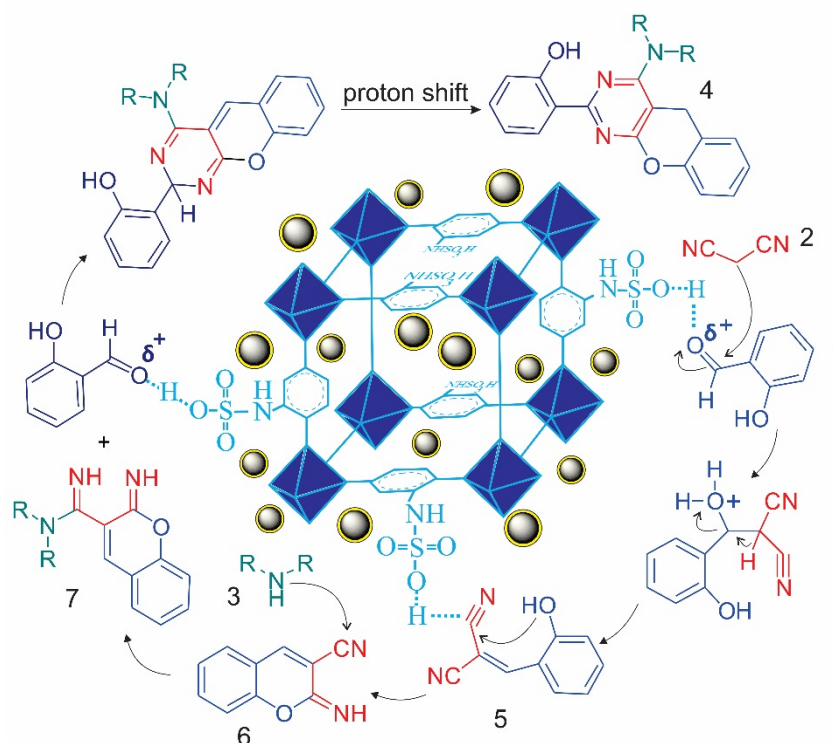
^c The yields of the model reaction with recycled catalyst after five successive runs.

To investigate the catalytic advantages of Fe₃O₄/IRMOF-3/SO₃H nanocomposite, a comparison table from previously reported data including yields and reaction conditions for pseudo four-component condensation reaction of salicylaldehyde, malononitrile, and morpholine (3j) is presented in Table 3. As a whole, the results demonstrate the benefits of the present protocol over some of the other former reported methods in terms of product yields, reaction times or reaction conditions.

Table 3. Comparison of the catalytic activity of Fe₃O₄/IRMOF-3/SO₃H with some of the other catalysts reported in the literature for the synthesis of 3j.

Entry	Catalyst	Conditions	Time (h)	Yield (%)	ref
1	Silica-bonded N-propylpiperazine sodium n-propionate	Solvent-free, rt	6	85	[47]
2	Fe(II)-BTU-SNPs	Ethanol, rt	4	93	[36]
3	Sodium formate	Ethanol, rt	12	83	[48]
4	Tetrabromobenzene-1,3-disulfonamide	Ethanol, rt	24	90	[49]
5	LiClO ₄	Ethanol, rt	24	84	[50]
6	Piperidine	MW, 100 C	0.1	92	[51]
7	[Hnhp][HSO ₄]	Solvent free, rt	0.2	87	[52]
8	Fe ₃ O ₄ /IRMOF-3/SO ₃ H	Ethanol, rt	1	95	This work

A proposed mechanism for the formation of the benzopyranopyrimidines with the aim of catalytic activity of Fe₃O₄/IRMOF-3/SO₃H is represented in Scheme 2. The Knoevenagel condensation reaction initiates with assistance of the Bronsted sulfamic acid sites (-SO₃H) through activation of the carbonyl group in salicylaldehyde towards nucleophilic attack of malononitrile. At the next step, the pinner reaction progress (5→6) through activating the triple bond with the aim of Bronsted acid sites, concluding in cyclization, in which continues by the amine attack to the activated intermediate 6. Finally, another salicylic aldehyde molecule interacts with the intermediate 7, following by proton transfer to achieve the benzopyranopyrimidine product.



Scheme 2. A proposed mechanism for synthesis of benzopyranopyrimidine through catalytic activation of Fe₃O₄/IRMOF-3/SO₃H nanocomposite

Conclusions

In summary, Fe₃O₄/IRMOF-3/SO₃H nanocomposite was synthesized through the post-modification of magnetic IRMOF-3 with chlorosulfonic acid, then was introduced for the synthesis of the benzopyranopyrimidines through one-pot multicomponent condensation reaction of secondary amines, malononitrile and salicylaldehydes under mild conditions. The magnetism with nanoparticles, besides post modification of IRMOF-3 with acidic groups produces a nanocomposite containing high potentials for catalytic application purposes. The Fe₃O₄/IRMOF-3/SO₃H nanocomposite was fully characterized and its stability was verified even after acidic treatment of the magnetic MOF with chlorosulfonic acid. The as-reported procedure contains some advantages such as accessible active Brønsted acid sites supported on high surface area magnetic MOF, applicability to a desired range of substituted salicylaldehyde and secondary amines, short reaction times, use of small amounts of catalytic resources, ease of separation, recycling and reusability of the catalyst, and simple reaction workup.

Experimental section

Materials and methods

All reagents with synthetic reagent grade were purchased from merck or sigma and used without further purification. The particle sizes and morphologies were studied by field emission scanning electron microscope (FE-SEM, MIRA3TESCAN-XMU with an accelerating voltage of 15 kV) equipped with an energy dispersive spectrometer (EDS) and an optical microscope (Nikon Eclipse LV 100). The Brunauer–Emmett–Teller (BET) surface area of the catalyst was investigated using a nitrogen adsorption instrument (Micrometrics ASAP 2020). Pore size was calculated using Density Functional Theory (DFT). Total pore volume was taken by a single point method at P/P₀ = 0.98. X-ray diffraction (XRD) was measured in a Philips PW 1730 instrument. FT-IR measurements were performed using KBr disc on a Thermo IR-100 infrared spectrometer (Nicolet). The thermogravimetric analysis (TGA) measurements were taken using SDT Q600. The acid capacities of the catalyst were determined by acid-base titration using NaCl solution as an ion-exchange agent.^[53] A 200 mg sample in powder form was ion-exchanged with an aqueous NaCl saturated solution at ambient temperature for at least 24 h, followed by filtration and washing with 3 mL of deionized (DI) water. The filtrates were then titrated with NaOH solution (0.01 M). The ¹H- and ¹³C-spectra were measured (CDCl₃) with a Bruker DRX 500-Avance FT-NMR instrument at 500.1 and 125.7 MHz, respectively.

Catalyst preparation

Synthesis of Fe₃O₄ nanoparticles

Initially Fe₃O₄ NPs were synthesized by a co-precipitation method.^[54] Briefly, a mixture of FeCl₂·4H₂O (10.8 mmol, 54.3 mg) and FeCl₃·6H₂O (21.6 mmol, 79.9 mg) were dissolved in distilled water (100 mL). Then, the reaction was continued under mechanical stirrer for 30 min at 85 °C in an argon atmosphere for homogeneity. Afterwards, ammonium hydroxide 25% (10 mL) was added in one portion into the reaction mixture, which immediately resulted in the formation of the magnetic black precipitates. The reaction was stirred for further 30 minutes, and then it was cooled to ambient temperature. The black as-prepared product was separated by an external magnetic decantation, washed several times with brine and distilled water, then was dried at 80 °C in vacuum, overnight.

Synthesis of Fe₃O₄@SiO₂ core-shell nanoparticles

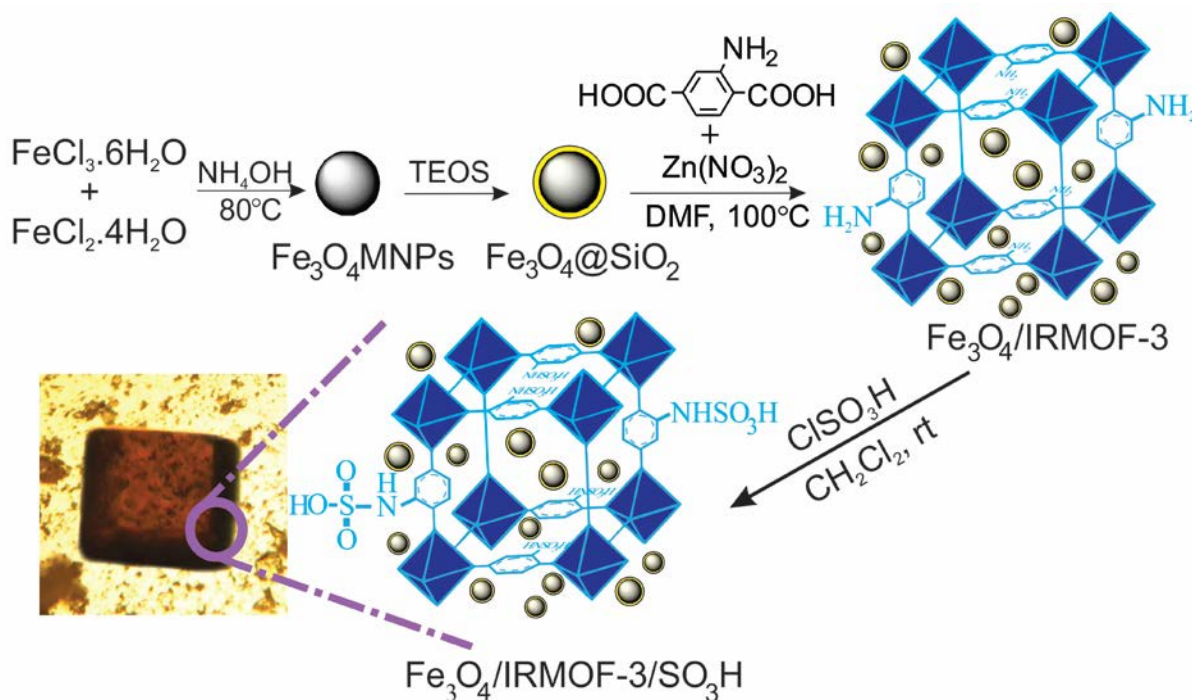
For preparation of the Fe₃O₄-SiO₂ core-shell; firstly, Fe₃O₄ NPs (1.0 g) were sonicated in an ethanol solution (150 mL). Then, ammonium hydroxide 25% (5 mL) was added to the magnetic dispersed solution and the reaction was stirred for 30 minutes. Subsequently, the Fe₃O₄ NPs were coated with SiO₂ through condensation and hydrolysis of 1 mL tetraethyl orthosilicate (TEOS), in which added dropwise into the reaction mixture over 10 minutes. The reaction was stirred vigorously for 24 h at room temperature. Finally, the obtained Fe₃O₄@SiO₂ NPs were collected by an external magnet, centrifuged and washed several times with DI water and ethanol, then dried in a vacuum oven at 80 °C for 24 h.

Synthesis of magnetic IRMOF-3 ($\text{Fe}_3\text{O}_4/\text{IRMOF-3}$)

Magnetic IRMOF-3 ($\text{Fe}_3\text{O}_4/\text{IRMOF-3}$) nanocomposite was obtained via a solvothermal method as follows: In a solution of $\text{Zn}(\text{NO}_3)_2$ (134 mg, 0.7 mmol) in pure DMF (8 mL), $\text{Fe}_3\text{O}_4@/\text{SiO}_2$ NPs (8 mg) were dispersed by sonication for 30 minutes. To the above mixture, 2-aminoterephthalic acid (33 mg, 0.18 mmol) was added and sonicated for another 10 minutes at room temperature. Subsequently, the dispersed mixture was transferred into a 50 mL Teflon-lined stainless steel autoclave and heated in stable conditions at 100 °C for 24 h. Finally, the obtained brownish precipitate was isolated by magnetic decantation and was washed several times with pure DMF and methanol, then dried in vacuum oven at 80 °C for 24 h.

Post-synthetic modification of $\text{Fe}_3\text{O}_4/\text{IRMOF-3}$ nanocomposite ($\text{Fe}_3\text{O}_4/\text{IRMOF-3}/\text{SO}_3\text{H}$)

The $\text{Fe}_3\text{O}_4/\text{IRMOF-3}$ (1g) was sonicated in CH_2Cl_2 (20 mL) for 30 minutes. Afterwards, chlorosulfonic acid (0.5 mL) was added dropwise to the reaction vessel under stirring over a period of 30 minutes and kept at room temperature, overnight. The obtained brownish precipitate was isolated by magnetic decantation and washed several times with pure CHCl_3 . For more activation, the nanocomposite was rinsed in 20 mL methanol twice in two days to remove all solvents trapped in pores. Finally, $\text{Fe}_3\text{O}_4/\text{IRMOF-3}$ was separated from methanol by magnetic decantation and dried at 90 °C under vacuum, for 24 h (Scheme. 3).



Scheme 3. Preparation of $\text{Fe}_3\text{O}_4/\text{IRMOF-3}/\text{SO}_3\text{H}$ nanocomposite.

General procedure for the preparation of benzopyranopyrimidines

In a screw cap test tube, a mixture of salicylaldehydes **1** (2 mmol), malononitrile **2** (1 mmol), secondary amines **3** (1 mmol) and $\text{Fe}_3\text{O}_4/\text{IRMOF-3}/\text{SO}_3\text{H}$ (10 mg) in EtOH (4 mL) was stirred at room temperature for 3 h. After completion of the reaction as monitored by TLC (eluent: EtOAc/n-hexane, 1:3), 10 mL hot ethanol was added and the catalyst was separated by magnetic decantation instantly. After cooling of the organic phase, the crude product was precipitated, then was filtered and washed with DI water and cold EtOH several times to afford the pure product.

Keywords: Magnetic metal-organic framework • Functionalized IRMOF-3 • Nanocomposite catalyst • Multicomponent reaction • Heterogeneous catalysis

- [1] R. W. Armstrong, A. P. Combs, P. A. Tempest, S. D. Brown, T. A. Keating, *Acc. Chem. Res.* **1996**, *29*, 123-131.
- [2] K. Kumaravel, G. Vasuki, *Curr. Org. Chem.* **2009**, *13*, 1820-1841.
- [3] S. Brauch, L. Gabriel, B. Westermann, *Chem. Commun.* **2010**, *46*, 3387-3389.
- [4] N. Elders, D. van der Born, L. J. D. Hendrickx, B. J. J. Timmer, A. Krause, E. Janssen, F. J. J. de Kanter, E. Ruijter, R. V. A. Orru, *Angew. Chem., Int. Ed.* **2009**, *48*, 5856-5859.
- [5] A. Dömling, *Chem. Rev.* **2006**, *106*, 17-89.
- [6] C. H. Cheon, H. Yamamoto, *Chem. Commun.* **2011**, *47*, 3043-3056.
- [7] F. C. Zheng, Q. W. Chen, L. Hu, N. Yan, X. K. Kong, *Dalton Trans.* **2014**, *43*, 1220-1227.
- [8] H. Veisi, A. Sedrpushan, A. R. Faraji, M. Heydari, S. Hemmati, B. Fatahi, *RSC Adv.* **2015**, *5*, 68523-68530.
- [9] S. K. Kundu, J. Mondal, A. Bhaumik, *Dalton Trans.* **2013**, *42*, 10515-10524.
- [10] M. B. Gawande, A. K. Rathi, I. D. Nogueira, R. S. Varma, P. S. Branco, *Green Chem.* **2013**, *15*, 1895-9.
- [11] Y. Chang, C. Bae, *Curr. Org. Synth.* **2011**, *8*, 208-236.
- [12] O. Z. Kwon, S. M. Park, G. Seo, *Chem. Comm.* **2007**, *40*, 4113-4115.
- [13] H. C. Zhou, S. Kitagawa, *Chem. Soc. Rev.* **2014**, *43*, 5415-5418.
- [14] J. Yu, L. H. Xie, J. R. Li, Y. Ma, J. M. Seminario, P. B. Balbuena, *Chem. Rev.* **2017**, *117*, 9674-9754.
- [15] L. J. Murray, M. Dinca, J. R. Long, *Chem. Soc. Rev.* **2009**, *38*, 1294-1314.
- [16] D. J. Xiao, E. D. Bloch, J. A. Mason, W. L. Queen, M. R. Hudson, N. Planas, J. Borycz, A. L. Dzubak, P. Verma, K. Lee, F. Bonino, V. Crocella, J. Yano, S. Bordiga, D. G. Truhlar, L. Gagliardi, C. M. Brown, J. R. Long, *Nat. Chem.* **2014**, *6*, 590-595.
- [17] Z. G. Gu, D. J. Li, C. Zheng, Y. Kang, C. Wöll, J. Zhang, *Angew. Chem., Int. Ed.* **2017**, *56*, 6853-6858.
- [18] J. Liu, T. Y. Bao, X. Y. Yang, P. P. Zhu, L. H. Wu, J. Q. Sha, L. Zhang, L. Z. Dong, X. L. Cao, Y. Q. Lan, *Chem. Comm.* **2017**, *53*, 7804-7807.
- [19] K. M. Park, H. Kim, J. Murray, J. Koo, K. Kim, *Supramol. Chem.* **2017**, *29*, 441-445.
- [20] J. Heine, K. M. Buschbaum, *Chem. Soc. Rev.* **2013**, *42*, 9232-9242.
- [21] J. J. Alcañiz, R. Gielisse, A. B. Lago, E. V. Ramos-Fernandez, P. S. Crespo, T. Devic, N. Guillou, C. Serre, F. Kapteijn, J. Gascon, *Catal. Sci. Technol.* **2013**, *3*, 2311-2318.
- [22] Y. Zang, J. Shi, F. Zhang, Y. Zhong, W. Zhu, *Catal. Sci. Technol.* **2013**, *3*, 2044-2049.
- [23] M. G. Goesten, J. J. Alcañiz, E. V. Ramos-Fernandez, K. B. Sai Sankar Gupta, E. Stavitski, H. Bekkum, J. Gascon, F. Kapteijn, *J. Catal.* **2011**, *281*, 177-187.
- [24] V. Valtchev, G. Majano, S. Mintova, J. Pérez-Ramírez, *Chem. Soc. Rev.* **2013**, *42*, 263-290.
- [25] R. S. Andriamitantoa, J. Wang, W. Dong, H. Gao, G. Wang, *RSC Adv.* **2016**, *41*, 35135-35143.
- [26] Y. Luan, N. Zheng, Y. Qi, J. Yu, G. Wang, *Eur. J. Inorg. Chem.* **2014**, *26*, 4268-4272.
- [27] L. M. Rossi, N. J. Costa, F. P. Silva, R. Wojcieszak, *Green Chem.* **2014**, *6*, 2906-2933.
- [28] O. Bruno, C. Brullo, S. Schenone, A. Ranise, F. Bondavalli, E. Barocelli, M. Tognolini, F. Magnanini, V. Ballabeni, *Il Farmaco* **2002**, *9*, 753-758.
- [29] O. Bruno, C. Brullo, S. Schenone, F. Bondavalli, A. Ranise, M. Tognolini, V. Ballabeni, E. Barocelli, *Bioorg. Med. Chem.* **2004**, *12*, 553-561.
- [30] O. Bruno, C. Brullo, A. Ranise, S. Schenone, F. Bondavalli, E. Barocelli, V. Ballabeni, M. Chiavarini, M. Tognolini, M. Impicciatore, *Bioorg. Med. Chem.* **2001**, *11*, 1397-1410.
- [31] O. Bruno, S. Schenone, A. Ranise, F. Bondavalli, E. Barocelli, V. Ballabeni, M. Chiavarini, S. Bertoni, *Bioorg. Med. Chem.* **2001**, *9*, 629-636.
- [32] A. K. Gupta, K. Kumari, N. Singh, D. S. Raghuvanshi, K. N. Singh, *Tetrahedron Lett.* **2012**, *53*, 650-653.
- [33] H. R. Shaterian, M. Aghakhanizadeh, *Res. Chem. Intermed.* **2013**, *39*, 3877-3885.
- [34] H. R. Tavakoli, S. M. Moosavi, A. Bazgir, *J. Korean Chem. Soc.* **2013**, *57*, 260-263.
- [35] S. M. Sadeghzadeh, F. Daneshfar, M. Malekzadeh, *Chin. J. Chem.* **2014**, *32*, 349-355.
- [36] S. Amirnejat, F. Movahedi, H. Masroui, M. Mohadesi, M. Z. Kassae, *J. Mol. Catal. A: Chem.* **2013**, *378*, 135-141.
- [37] M. M. Mostafavi, F. Movahedi, *Appl. Organomet. Chem.* **2018**, *32*, e4217-e4227.
- [38] F. Movahedi, H. Masroui, M. Z. Kassae, *J. Mol. Catal. A: Chem.* **2014**, *395*, 52-57.
- [39] Y. Jiang, J. Jiang, Q. Gao, M. Ruan, H. Yu, L. Qi, *Nanotechnology* **2008**, *19*, 75714-75719.
- [40] F. X. L. Xamena, A. Abad, A. Corma, H. Garcia, *J. Catal.* **2007**, *250*, 294-298.
- [41] F. X. L. Xamena, F. G. Cirujano, A. Corma, *Micropor. Mesopor. Mater.* **2012**, *157*, 112-117.
- [42] S. Rostamnia, H. Xin, N. Nouruzi, *Micropor. Mesopor. Mater.* **2013**, *179*, 99-103.
- [43] S. Huo, X. P. Yan, *Analyst* **2012**, *137*, 3445-3451.
- [44] Y. J. Kim, D. W. Park, *J. Nanosci. Nanotechnol.* **2013**, *13*, 2307-2312.
- [45] R. M. Cornell, U. Schwertmann, *The Iron Oxides*, VCH, New York, **1996**.
- [46] A. Zonouzi, F. Hosseinzadeh, N. Karimi, R. Mirzazadeh, S. W. Ng, *ACS Comb. Sci.* **2013**, *15*, 240-246.
- [47] K. Niknam, N. Borazjani, *Monatsh. Fur. Chemie.* **2016**, *147*, 1129-1135.
- [48] G. Brahmachari, S. Das, *J. Heterocycl. Chem.* **2015**, *52*, 653-659.

- [49] R. Ghorbani-Vaghei, M. Shirzadi-Ahodashi, F. Eslami, S. M. Malaekhepoor, Z. Salimi, Z. Toghraei-Semiromi, S. Noori, *J. Heterocycl. Chem.* **2017**, *54*, 215-225.
- [50] R. Ghahremanzadeh, T. Amanpour, A. Bazgir, *Tetrahedron Lett.* **2010**, *51*, 4202-4204.
- [51] O. Bruno, C. Brullo, F. Bondavalli, A. Ranise, S. Schenone, M. Tognolini, V. Ballabeni, E. Barocelli, *Med. Chem.* **2007**, *3*, 127-134.
- [52] A. Zonouzi, M. Biniiaz, R. Mirzazadeh, *Heterocycles* **2010**, *81*, 1271-1278.
- [53] S. Y. Chen, T. Yokoi, C. Y. Tang, L. Y. Jang, T. Tatsumi, J. C. Chan, S. Cheng, *Green Chem.* **2011**, *13*, 2920-2930.
- [54] X. Liu, Z. Ma, J. Xing, H. Liu, *J. Mag. Mater.* **2004**, *270*, 1-6.